ACADEMIA
MATERIALS SCIENCE

Research Article
Published: 2025-02-26
https://doi.org/10.20935/AcadMatSci7554

In situ synthesis and AC conductivity studies of polypyrrole–cobalt nanocomposites

Revanasiddappa Moolemane[1], Honnalagere Mahadevaswamy Rashmi[2], Mavalangi Surekha[2], Suresh Babu Naidu Krishna[3,4,*]

Academic Editor: Raul D.S.G. Campilho

Abstract

Through in situ pyrrole chemical polymerization with various concentrations of $CoCl_2$, conducting polypyrrole-cobalt composites were synthesized using ammonium persulfate as the oxidizing agent. These composites were synthesized using different molarities (0.01, 0.02, 0.03, and 0.05 M) of $CoCl_2$ in polypyrrole. The PPy-Co nanocomposites and their AC conductivity studies were evaluated in this study. The formation of nanocomposites and the structural properties of PPy/PVA/Co were confirmed using FTIR analysis and X-ray crystallography. Scanning electron microscopy (SEM) was used to analyze the morphology of the composites, and thermogravimetric analysis (TGA) was used to investigate their thermal behavior. The room-temperature AC conductivity and dielectric response of the composites were investigated, and frequency-dependent AC conductivity investigations were conducted in the frequency range of 100 Hz–1 MHz.

Keywords: *polypyrrole, cobalt chloride, nanocomposite, AC conductivity, dielectric studies*

Citation: Moolemane R, Rashmi HM; Surekha M, Krishna SBN. In situ synthesis and AC conductivity studies of polypyrrole–cobalt nanocomposites. *Academia Materials Science* 2025;2. https://doi.org/10.20935/AcadMatSci7554

1. Introduction

Polymer nanocomposites have excellent physical and mechanical characteristics compared to host polymers, partially due to the large interfacial region between polymers and nanofillers. To overcome some of the limitations of polymers and hence widen their applications, fillers of different sizes are frequently used as reinforcements for polymers [1]. Polymer composites are special in terms of their physical and chemical characteristics, including flexibility, tensile strength, toughness, and electrical conductivity. Polymers with conjugated single and double bonds that aid in conduction are known as conducting polymers [2]. Polyaniline, polypyrrole, polyacetylene, and polythiophene are the most studied intrinsic conducting polymers for applications in sensors, EMI shielding, supercapacitors, and electronics [3–5]. Owing to its simple synthesis, economic viability, and intriguing chemical characteristics, polypyrrole (PPy) has been the subject of most research on conducting polymers [6, 7]. The application of polypyrrole and its composite materials in solar cells, coating materials, biosensors, actuators, artificial muscles, electromagnetic radiation shielding materials, and corrosion inhibitors is widespread [8, 9]. The size management of PPy nanoparticles has been investigated, and it was found that PPy nanoparticles can be successfully dispersed because of their high surface area and significant conductivity.

In this study, PPy-Co nanocomposites were synthesized via in situ polymerization using polyvinyl alcohol as the binder matrix and ammonium persulfate as the oxidizing agent. The effect of PPy on the nanocomposites was also analyzed by varying the Co concentration while maintaining the PPy concentration. The chemical composition of the PPy-PVA-Co composites was examined using X-ray diffraction (XRD) and Fourier transform infrared spectroscopy (FTIR), while scanning electron microscopy (SEM) was employed to examine the shape of the composites. The thermal characteristics of the resulting composites were assessed using thermogravimetric analysis (TGA). Finally, in addition to the thermal stability, the synergetic conductivity impact of PPy with Co was investigated.

2. Materials and methods

2.1. Materials

Poly vinyl alcohol (PVA) and cobalt chloride were used as the starting materials. Pyrrole (99% analytical grade) was acquired from Sigma-Aldrich, vacuum-distilled, and stored at 5 °C before use. The synthesis was conducted using distilled water. To synthesize the PPy-Co nanocomposites, ammonium persulfate was used as the oxidizing agent via in situ polymerization. Dried *Adathoda vasica* leaves were obtained from a local market. Solvents were obtained from S.D Fine-Chem (Bangalore, India). Fine compounds were obtained from Sigma-Aldrich (India). A programmable computer-interfaced digital LCR meter (Hioki (model 3532), Nagano, Japan) was used to measure the frequency-dependent AC conductivity of

[1]Department of Chemistry, PES University, Electronic City Campus, Hosur Road, Bangalore 560 100, Karnataka, India.
[2]VTU-Belagvi, Research Centre-Department of Chemistry, The Oxford College of Engineering, Hosur Road, Bangalore 560068, Karnataka, India.
[3]Faculty of Health Sciences, Durban University of Technology, Durban 4000, South Africa.
[4]School of Life Sciences, University of KwaZulu-Natal, Westville Campus, Durban 4000, South Africa.
*email: sureshk@dut.ac.za or suresh.nrdc@gmail.com

PPy-Co nanocomposites in the selected frequency range of 10^2–10^7 Hz at room temperature.

2.2. Synthesis of PPy-Co nanocomposites

PVA (10 g) was dissolved in 100 mL of distilled water, and the mixture was vigorously stirred using a magnetic stirrer for two hours on a hot plate to create a transparent, homogenous PVA solution. Carefully weighed molarities of $CoCl_2$ (0.01, 0.02, 0.03, and 0.05 M) were dissolved in distilled water in separate beakers. Adathoda vasica leaves (5 g) were boiled for ten minutes in 200 mL of distilled water before being filtered to create an extract. The PPy-PVA–Adathoda leaf extract–Co nanocomposite was created by the in situ polymerization of pyrrole in the presence of PVA, *Adathoda leaf* extract, and a colloidal solution of cobalt nanoparticles. Ammonium persulfate was added as an oxidant, kept in a cold bath, and subjected to constant stirring for an hour. The mixture was blended with the PVA solution and dried using a Buchner funnel to produce an evenly black wet product. *Adathoda vasica* is a medicinal plant traditionally used to treat asthma. This plant contains polyphenols, which act as reducing agents, helping to reduce silver ions into silver nanoparticles. The presence of these nanoparticles in the conducting polymer matrix has been confirmed through XRD and IR analyses. Conductivity is further enhanced by incorporating cobalt (Co) nanoparticles into the PVA matrix. The obtained conductive films confirm the presence of nanoparticles through AC conductivity measurements and EMI shielding effectiveness studies.

2.3. Characterization of the samples

A Cu Kα source was used to obtain the X-ray diffraction (XRD) spectra of the PVA and PPy-Co nanocomposites. The samples were scanned at a rate of 1.1° min^{-1} and had λ = 1.541 Å in the Bragg angle range of 2θ = 10–80°. The FTIR spectra of the PVA and PPy-Co nanocomposites were acquired in the 400–4000 cm^{-1} range using a Nicolet 750 FT-IR spectrometer (USA). With a Quanta 3D FEG apparatus, the morphological structures of the PVA and PPy-Co nanocomposites were captured by scanning electron microscopy (SEM).

2.4. AC response measurements

Using a Hioki model 3532-50 (Japan) programmed computer-interfaced digital LCR meter in the chosen frequency range of 100 Hz–1 MHz, the AC frequency response of the PVA and PPy-Co nanocomposite samples (in the form of cylindrical pellets with silver electrodes) was measured.

3. Results and discussions

3.1. FTIR studies

The FTIR spectra of PVA and the PVA/PPy/Co composites were examined in the range 4000–500 cm^{-1} (**Figure 1**). The FTIR profile of the PVA polymer exhibits peaks at approximately 3200 and 2880 cm^{-1}, indicative of O-H and C-H stretching, respectively [10]. The IR band around 640 cm^{-1} also supports the presence of a hydroxyl group. The spectral band observed around 3200–3800 cm^{-1} could be attributed to the -NH and-OH stretching frequencies of PPY and PVA, respectively. A shift in the PVA spectral bands could result from both Co doping and the formation of the PVA/PPY composite, as reported for the 2880 band shifting to higher values as a result of the interaction between PVA and PPY [11]. More importantly, the peak at ~1650 cm^{-1} corresponds to the carbonyl C=O group of PVA [12], after which the carbonyl C=O group is diminished or shifted. The negligible spectral band around 1537 cm^{-1} could be due to the -C=N vibration of the PPY molecules [13].

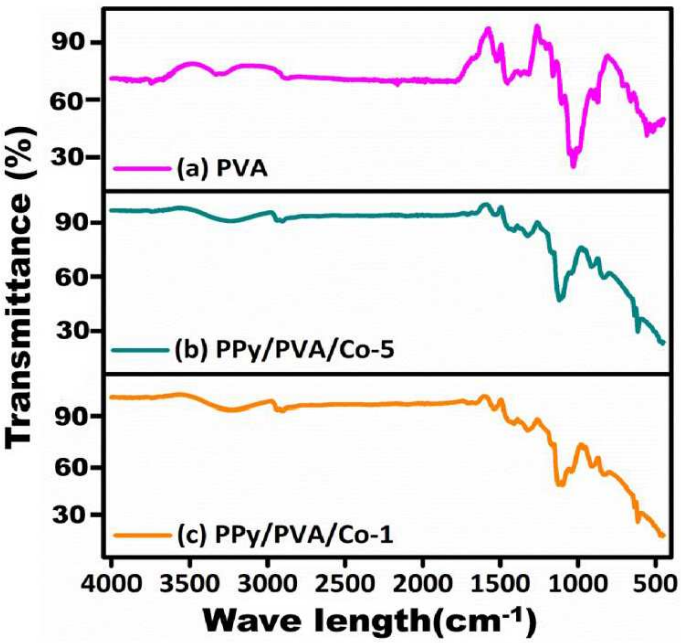

Figure 1 • FTIR spectra of (**a**) PVA, (**b**) PPy/PVA/Co-5, and (**c**) PPy/PVA/Co-1 nanocomposites.

3.2. XRD studies

The XRD patterns of PVA and the PVA/PPy/Co composite are shown in **Figure 2**. The XRD patterns of pure PVA display a large crystalline peak at 2θ of approximately 22° and a shoulder peak at approximately 25°, which correspond to the 101 and 200 planes of the monoclinic crystal structure, respectively. Because of the strong intermolecular H-bonding interactions within the PVA chain, PVA may have a semicrystalline structure. Notably, the characteristic diffraction peaks for PPy are negligible or null owing to their non-crystalline and amorphous nature [14]. Following the addition of the dopant (Co), decreasing the particle size increases the amorphous content. The polymer matrix (PVA) containing polypyrrole increases the amorphous nature, resulting in broad peaks in the XRD patterns. The XRD patterns of the composite films show that they are amorphous in nature. The diffraction peak intensity progressively decreases with increasing Co concentration because of the interaction between PVA/PPy, and the Co reduces the degree of crystallinity and intermolecular interactions between the PPy/PVA chains [10].

3.3. TGA studies

The thermal behavior of the PVA and PVA/PPy/Co composites was analyzed by thermogravimetric analysis (TGA) (**Figure 3**). In an N_2 environment, the thermal stability of the produced PVA and PVA/PPy/Co composites was examined up to 450 °C at a heating rate of 10 °C/min. The loss of absorbed water molecules

is evident in the first stage, which occurs between 100 °C and 250 °C. Water bound to the polymer matrix may be lost in the second stage of weight loss, which occurs between 250 °C and 350 °C. The breakdown and carbonization of PVA are attributed to the third stage, which occurs between 350 °C and 450 °C [15]. In the composite PVA/PPy/Co sample, the degradation of the PPy chain may contribute to the second stage of weight loss, which occurs between 250– and 350 °C and begins with the loss of absorbed water molecules [11]. However, the total weight loss in the PVA/PPy/Co composite may be as low as ~59 wt%, whereas the total weight loss in pure PVA is estimated to be as much as 85 wt%.

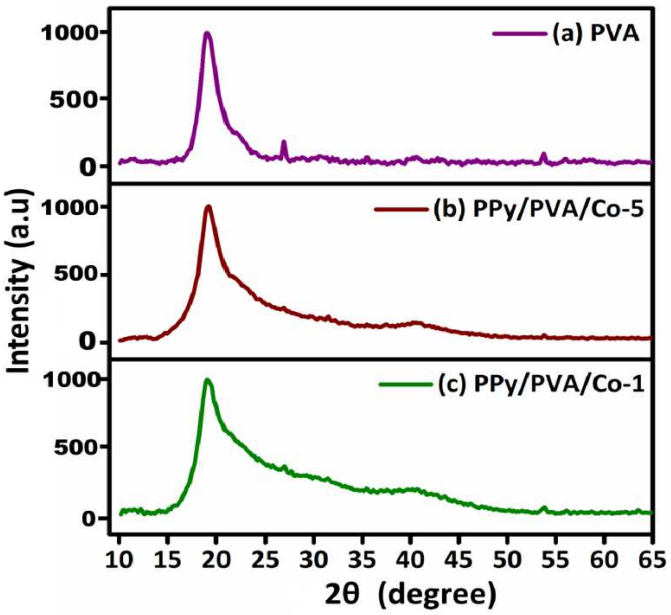

Figure 2 • XRD pattern of (**a**) PVA, (**b**) PPy/PVA/Co-5, and (**c**) PPy/PVA/Co-1 nanocomposites.

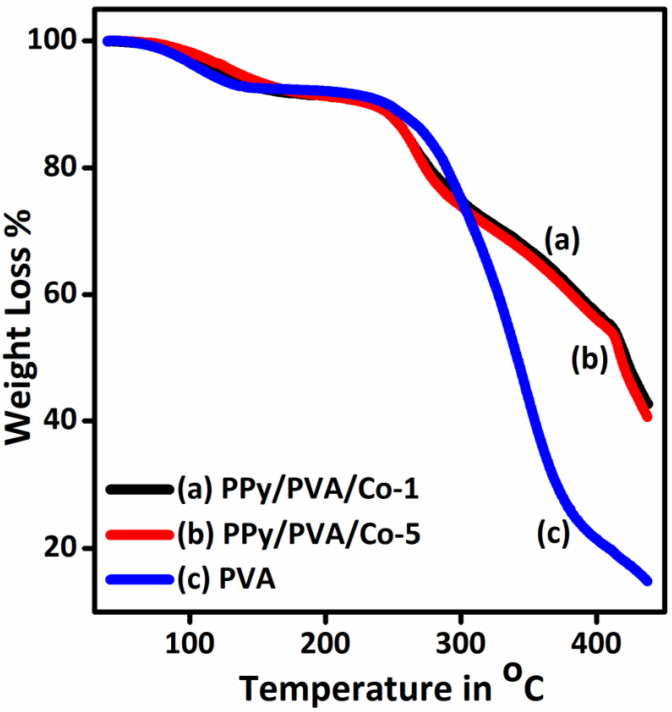

Figure 3 • TGA curve of (**a**) PPy/PVA/Co-1, (**b**) PPy/PVA/Co-5, and (**c**) PVA nanocomposites.

3.4. SEM studies

SEM images of PVA and PVA/PPy/Co composites are shown in **Figure 4**. The aggregated layered surface of the pristine PVA film is visible in the SEM images. However, if we pay close attention, the porosity morphology is uneven, and the PVA molecules are primarily grouped. In the case of PVA/PPy/Co, a clear composite formation can be seen. In the SEM images of the composite, the aggregated morphology of Co nanoparticles, along with the PVA polymer matrix and PPy nanofibers, can be observed (**Figure 4b,c**). The Co nanoparticles are in the range of 500 nm^{-1} μm. A 0.01 M concentration of Co nanoparticles shows an increase in conductivity, clearly indicating the formation of a conductive path in the film. However, as the concentration of Co nanoparticles increases further, conductivity decreases due to the creation of obstacles that hinder polaron hopping within the matrix. The same is confirmed through SEM images.

3.5. AC conductivity studies

Figure 5 exhibits the AC conductivity vs. frequency plots of PVA and PPy/PVA/Co nanocomposites. This clearly indicates that the conductivity increases as the cobalt content increases. This indicates that an increase in Co concentration results in increased polaron density. However, the conduction process in these composites seems to increase with the applied frequency after a particular frequency known as the critical frequency [16]. The low-frequency behavior of all the composites (up to 10^4 Hz) appears to follow a straight-line characteristic [17]. This might be because an increase in frequency increases the polaron-hopping frequency [18]. Owing to the Debye-like relaxation mechanism, the composite with PPy/PVA/Co-1 exhibited the maximum value of σ_{ac}. This could be a result of the variability in the distribution of Co particles, which might allow more charge carriers to hop between favorable localized spots, leading to an increase in conductivity. As the concentration of Co nanoparticles in the polymer matrix increases, the conductivity decreases. This reduction is attributed to the orientation polarization of molecules in the conducting polymer matrix. However, incorporating 0.1 M of Co nanoparticles into the conducting polymer matrix enhances conductivity, particularly with an increase in frequency. A modification in the electrical response was observed due to the addition of Co nanoparticles in the Ppy/PVA matrix due to the formation of agglomerates, crosslinks, and conductive paths, which are favorable for electrical conduction in these composites. The plots indicate a low-frequency plateau zone in PPy/PVA/Co and all composite samples up to 10^4 Hz, where DC conduction predominates. After this frequency, conductivity sharply increases, which is a feature of disordered systems.

3.6. Dielectric studies

The real component of the dielectric constant (ε') for PVA and PPy/PVA/Co nanocomposites varies with frequency (f), as shown in **Figure 6**. The dielectric constant continuously decreases with increasing frequency until it approaches a constant value at high frequencies. The low-frequency tendency of the macromolecular dipoles to align themselves with the applied field could account for this. Because dipoles are unable to orient themselves in the direction of the applied field, the dielectric constant is nearly constant in the high-frequency zone [19]. Maxwell–Wagner–Sillars polariza-

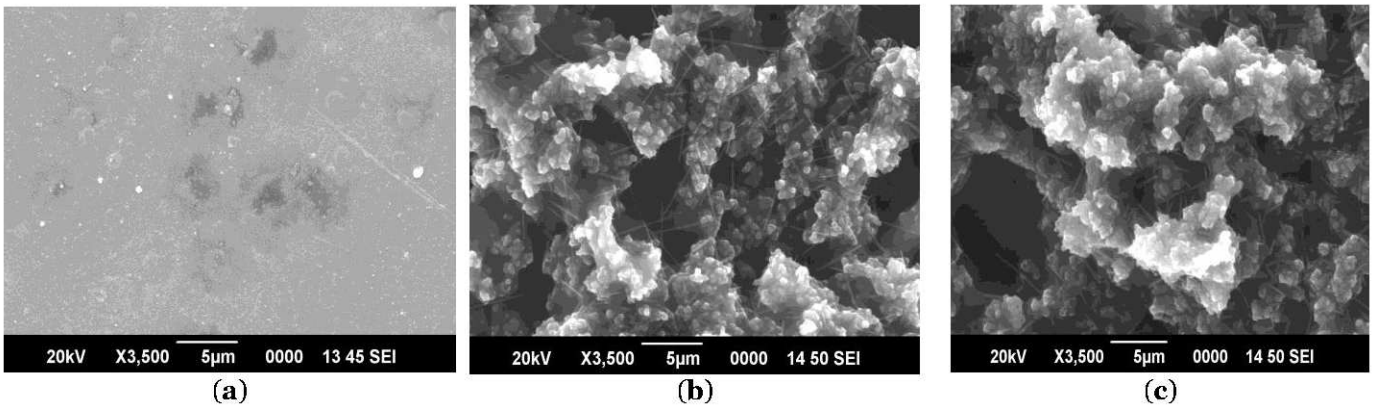

Figure 4 • SEM images of (**a**) PVA, (**b**) PPy/PVA/Co-1, and (**c**) PPy/PVA/Co-5 nanocomposites.

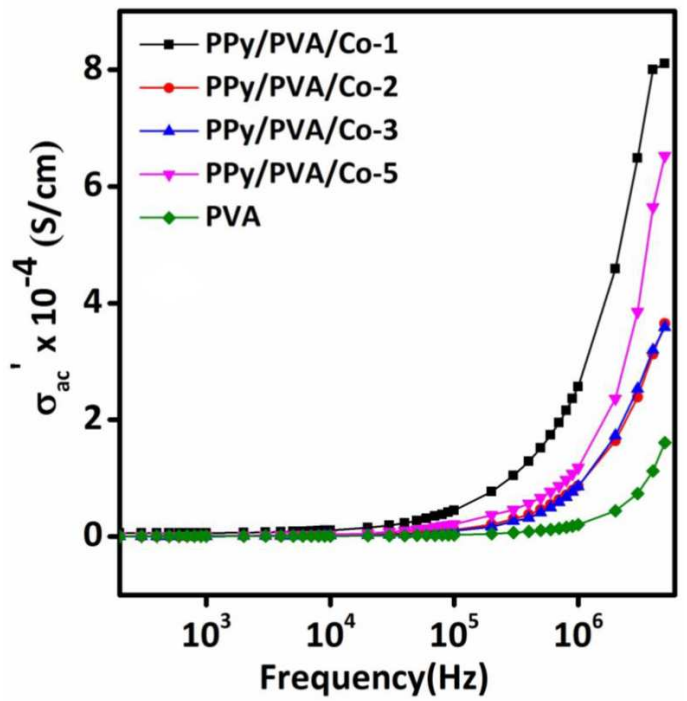

Figure 5 • Variation in AC conductivity with the frequency of PVA and different concentrations of PPy/PVA/Co nanocomposites.

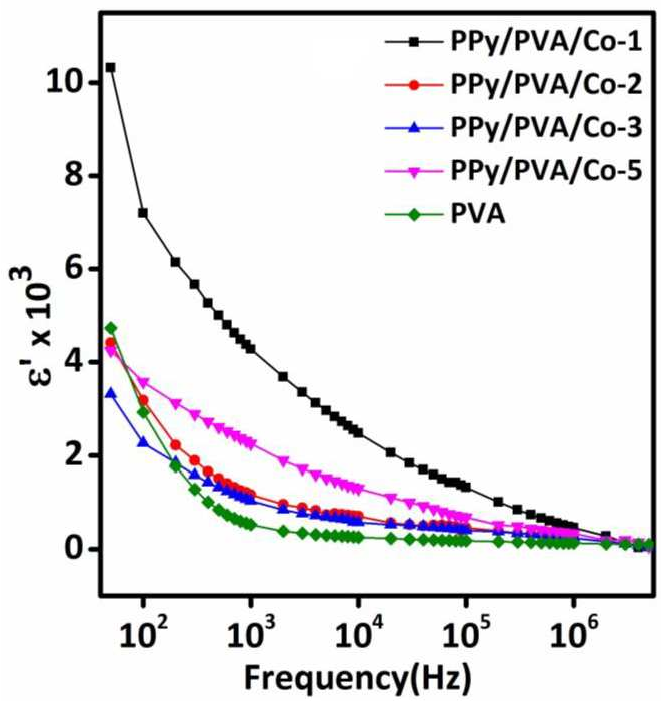

Figure 6 • Frequency dependence of the dielectric constant of PVA and various concentrations of PPy/PVA/Co nanocomposites.

tion in the nanocomposites was facilitated by the uniform distribution of the nanomaterial. However, at higher loadings, the non-homogenous morphology constrained the direction of the dipoles, resulting in a decrease in the dielectric constant values [20]. As the concentration of Co nanoparticles in the polymer matrix increases, the dielectric constant decreases under higher frequencies because dipoles are unable to orient themselves in the direction of the applied frequency. This reduction is attributed to the space polarization of molecules in the conducting polymer matrix. However, incorporating 0.1 M of Co nanoparticles into the conducting polymer matrix enhances the dielectric constant, particularly with an increase in frequency to a certain extent.

4. Conclusions

The synthesis, dielectric characterization, and conductivity of the PPy/PVA/Co (0.01, 0.02, 0.03, and 0.05 M) are reported in this study. An effective technique for creating polypyrrole–cobalt nanocomposites is in situ chemical oxidative polymerization. The differences in the structural phase of the nanocomposite are indi-cated by XRD. The FTIR spectra confirm that Co nanoparticles are present in the polymer nanocomposites. TGA shows the changes in the melting and decomposition temperatures of the PPy nanocom-posites. According to structural and morphological analyses, the PPy/PVA/Co nanocomposites exhibit better porous, granular, and globular surface morphologies with outstanding homogeneity and adhesiveness. The AC conductivity of the synthetic polymer composites displays Debye-type single relaxation and follows the power law index. On the other hand, the true dielectric values decrease with increasing frequency, suggesting that conduction charges play a role in the dielectric response.

Acknowledgments

The authors would like to express their gratitude to the management of PES University, Electronic City Campus, Bangalore, and the Vision Group on Science and Technology for their support in carrying out this research work under the grant PESUIRF/Chemistry-ECC/2020/14 dated 30-09-2020. KSBN would like to thank the Durban University of Technology for its research fellowship.

Funding

No funding was received to assist with the preparation of this manuscript.

Author contributions

R.M.: conceptualization, supervision, data curation, formal analysis, and writing—original draft and review. H.M.R.: data curation, formal analysis, and writing—original draft. M.S.: data curation, formal analysis, and writing—original draft. S.B.N.K.: formal analysis, data curation, resources, visualization, and writing—review and editing. All authors have read and agreed to the published version of the manuscript.

Conflict of interest

All authors certify that they have no affiliations with or involvement in any organization or entity with any financial interest or non-financial interest in the subject matter or materials discussed in this manuscript.

Data availability statement

Data supporting these findings are available within the article, at https://doi.org/10.20935/AcadMatSci7554, or upon request.

Institutional review board statement

Not applicable.

Informed consent statement

Not applicable.

Additional information

Received: 2024-11-22

Accepted: 2025-02-12

Published: 2025-02-26

Academia Materials Science papers should be cited as *Academia Materials Science 2025*, ISSN 2997-2027, https://doi.org/10.20935/AcadMatSci7554. The journal's official abbreviation is *Acad. Mat. Sci.*

Publisher's note

Copyright

References

1. Gunjal LB, Manjunatha S, Chethan B, Nagabhushana NM, Ravikiran YT, Machappa T, et al. Humidity sensing performance of polyaniline—Neodymium oxide composites. MRS Commun. 2023;13:248–55. doi: 10.1557/s43579-023-00336-3

2. Manjunatha S, Machappa T, Ravikiran YT, Chethan B, Sunilkumar A. Polyaniline based stable humidity sensor operable at room temperature. Phys B Condens Matter. 2019;561:170–8. doi: 10.1016/j.physb.2019.02.063

3. Manjunatha S, Machappa T, Ravikiran YT, Chethan M, Revanasiddappa M. Room temperature humidity sensing performance of polyaniline—Holmium oxide composite. Appl Phys A. 2019;125:361. doi: 10.1007/s00339-019-2638-1

4. Manjunatha S, Chethan B, Ravikiran YT, Machappa T. Room temperature humidity sensor based on polyaniline- tungsten disulfide composite. AIP Conf Proc. 2018;1953:030096-1–030096-4. doi: 10.1063/1.5032431

5. Vinay K, Revanasiddappa M, Manjunatha S, Shivakumar K, Ravikiran YT. Room temperature humidity sensing behaviour of silver decorated polyaniline composite. Mater Res Express. 2019;6:104003. doi: 10.1088/2053-1591/ab3624

6. Megha R, Ravikiran YT, Kumari SCV, Prakash HGR, Revanasiddappa M, Manjunatha S, et al. Structural and electrical characterization studies for ternary composite of polypyrrole. J Mater Sci Mater Electron. 2020;31:18400–11. doi: 10.1007/s10854-020-04386-4

7. Patel BMB, Revanasiddappa M, Rangaswamy DR, Manjunatha S, Ravikiran YT. DC conductivity studies of iron decorated polypyrrole. J Phys Conf Ser. 2021;2070:012070. doi: 10.1088/1742-6596/2070/1/012070

8. Megha R, Ravikiran YT, Kumari SCV, Rajprakash HG, Manjunatha S, Revanasiddappa M, et al. AC conductivity studies in copper decorated and zinc oxide embedded polypyrrole composite nanorods: Interfacial effects. Mater Sci Semicond Process. 2020;110:104963. doi: 10.1016/j.mssp.2020.104963

9. Patel BMB, Revanasiddappa M, Rangaswamy DR, Manjunatha S, Ravikiran YT. Electrical conductivity and EMI shielding studies of iron-decorated polypyrrole-fly ash nanocomposites. Mater Today Proc. 2021;49(Pt5):2253–9. doi: 10.1016/j.matpr.2021.09.337

10. Elkomy GM, Mousa SM, Mostafa HA. Structural and optical properties of pure PVA/PPY and cobalt chloride doped PVA/PPY films. Arab J Chem. 2016;9:S1786–92. doi: 10.1016/j.arabjc.2012.04.037

11. Das M, Sarkar D. Development of room temperature ethanol sensor from polypyrrole (PPy) embedded in polyvinyl alcohol (PVA) matrix. Polym Bull. 2018;75:3109–25. doi: 10.1007/s00289-017-2192-y

12. Makled MH, Sheha E, Shanap TS, El-Mansy MK. Electrical conduction and dielectric relaxation in p-type PVA/CuI polymer composite. J Adv Res. 2013;4:531–8. doi: 10.1016/j.jare.2012.09.007

13. Sunilkumar A, Manjunatha S, Chethan B, Ravikiran YT, Machappa T. Polypyrrole–Tantalum disulfide composite: An efficient material for fabrication of room temperature operable humidity sensor. Sens Actuators A Phys. 2019;298:111593. doi: 10.1016/j.sna.2019.111593

14. Sunilkumar A, Manjunatha S, Machappa T, Chethan B, Ravikiran YT. A tungsten disulphide–polypyrrole composite-based humidity sensor at room temperature. Bull Mater Sci. 2019;42:271. doi: 10.1007/s12034-019-1955-5

15. Gomaa MM, Hugenschmidt C, Dickmann M, Abdel-Hady EE, Mohamed HFM, Abdel-Hamed MO. Crosslinked PVA/SSA proton exchange membranes: Correlation between physiochemical properties and free volume determined by positron annihilation spectroscopy. Phys Chem Chem Phys. 2018;20:28287–99. doi: 10.1039/C8CP05301D

16. Manjunatha S, Machappa T, Sunilkumar A, Ravikiran YT. Tungsten disulfide: an efficient material in enhancement of AC conductivity and dielectric properties of polyaniline. J Mater Sci Mater Electron. 2018;29:11581–90. doi: 10.1007/s10854-018-9255-1

17. Manjunatha S, Sunilkumar A, Ravikiran YT, Machappa T. Effect of holmium oxide on impedance and dielectric behavior of polyaniline–holmium oxide composites. J Mater Sci Mater Electron. 2019;30:10332–41. doi: 10.1007/s10854-019-01371-4

18. Sunilkumar A, Manjunatha S, Ravikiran YT, Revanasiddappa M, Prashantkumar M, Machappa T. AC conductivity and dielectric studies in polypyrrole wrapped tungsten disulphide composites. Polym Bull. 2021;79:1391–407. doi: 10.1007/s00289-021-03552-w

19. Manjunatha S, Megha R, Chethan B, Prashantkumar M, Ravikiran YT, Machappa T. Structural and AC Electrical Properties of Tantalum Disulfide Embedded Polyaniline Composites. J Mater Eng Perform. 2021;30:1885–94. doi: 10.1007/s11665-021-05526-5

20. Kumar AS, Manjunatha S, Ravikiran YT, Devendrappa H, Machappa T. AC frequency-dependent dielectric studies of polypyrrole composites. AIP Conf Proc. 2020;080005:080005-1–080005-4. doi: 10.1063/5.0009037